Available online at www.sciencedirect.com

ScienceDirect

Ceramics International 40 (2014) 10677–10684

CERAMICS INTERNATIONAL

www.elsevier.com/locate/ceramint

Comparative microstructure study of high strength alumina and bauxite insulator

Yong Meng[a,b], Guohong Gong[b,*], Dongtian Wei[a,b], Yumin Xie[c], Zongju Yin[c]

[a]University of Chinese Academy of Sciences, Beijing 100049, China
[b]State Key Laboratory of Ore Deposit Geochemistry, Institute of Geochemistry, Chinese Academy of Sciences, Guiyang 550002, Guizhou, China
[c]Bijie Highland Porcelain Insulator Limited Liability Company, Bijie 551700, Guizhou, China

Received 8 February 2014; received in revised form 7 March 2014; accepted 7 March 2014
Available online 27 March 2014

Abstract

The property of insulators is closely related to microstructures. In order to study the difference and similarity of two kinds of insulators microstructure and thereby explore ways to improve the property of insulators further, a comparative study was carried out on three high strength porcelain insulators by XRD, SEM and ceramography. The results indicate that there exists a negative linear relationship between the porosity and the content of amorphous phase. Porosity is the main factor affecting the density of insulator body. Compared with alumina, the calcined bauxite used as raw material will cause the increase of porosity. Microcracks usually appear in vitrified area and area around quartz particle where mullite is rare, crack is obvious. Decreasing the amount of quartz in raw material and increasing the amount of mullite in vitrified area could improve the mechanical strength of porcelain insulators further.

Keywords: E. Insulator; Microstructure; Composition; Comparison

1. Introduction

Insulators are essential components widely used on power transmission and distribution network [1–3]. They are fabricated by means of a series of minerals such as kaolinite and feldspar going through a complicated process and then sintered under given heating procedure. They have two basic functions: fastening mechanically and insulating electrically the active components of electric network [4,5]. As an eligible insulator, it is required to have high resistivity, high dielectric strength, low loss factor, good mechanical strength, excellent in heat radiation and insulating components even in humid or corrosive situation [5–7].

The porcelain insulator is one of the three kinds of insulators, i.e., porcelain insulator, glass insulator and composite insulator, which possesses all the properties required as an eligible insulator [8]. Porcelain insulators, having been put into application more than 160 years since 1850 when insulators were introduced in the construction of power transmission network by Werner Von Siemens, are the most prevalent insulators [2,6,9]. For porcelain insulators, there are several excellent properties (e.g. high mechanical strength, high resistance and corrosion resistance), which could not be realized in other materials simultaneously [2,6,10].

With increasing requirement on the strength level of porcelain insulators in the field of electrical engineering, porcelain insulators have undergone a development from feldspar insulators to cristobalite insulators, and finally to alumina/bauxite insulators [2,6]. The alumina insulators are such kind of product in the formulation of which industrial alumina is added as a dispersion strengthen phase, while that for the bauxite insulators calcined bauxite is added as dispersion strengthen phase. From the point of cost and resource, bauxite insulators are cost saving and rich in resource than alumina insulators, which is the advantage of bauxite insulators [2,6].

The property of insulators after sintering is depending on many aspects: the constituent phases resulting from high temperature reaction involving the mineral used; the microstructure formed in

*Corresponding author. Tel./fax: +86 851 5891606.
E-mail address: gongguohong@vip.gyig.ac.cn (G. Gong).

http://dx.doi.org/10.1016/j.ceramint.2014.03.052
0272-8842/

the body; the degree of densification; and the amount of detrimental chemical composition remained in the body after sintering. Among the factors mentioned above, microstructures determine the mechanical property of final products to a considerable degree [11]. When it comes to the concept of microstructures, it includes many aspects of material, such as type and amount of phases existing in the body as well as their shape, size, orientation and distribution. For ceramic material, microstructures mean all parameters and data describing a given material. Crystallite components, particle size, particle shape, porosity, melted phase and texture are essential characteristics of microstructures [6,12].

Before putting into application, insulators must get the qualification certificate issued by IEC, which involve many property tests (e.g. electromechanical failure load test, flash test, power frequency sparking test, more details in IEC 60383-1:1993 MOD standard), having been accepted generally in the field of insulator fabrication [2]. For the purpose of safety, the IEC property tests are really strict, and this is why it is difficult to get the qualification certificate. The electromechanical failure load is one of the most important properties of insulators. Hence, the electromechanical failure load is taken as the grading standard of insulators. In brief, the electromechanical failure load test is performing on samples with a tensile tester accompanying a given power frequency voltage until destroyed. The electromechanical failure load (E) is expressed as follows:

$$E = \bar{E} - 3\sigma \quad (1)$$

where $\bar{E}$ is the average electromechanical failure load and σ is the standard deviation.

According to the electromechanical failure load grading standard, insulators could be divided into 100 kN level, 200 kN level, 300 kN level, 400 kN level and 500 kN level.

In the present work, a comparative study was performed on the type and amount of three 400 kN level insulator microstructures as well as their size, shape and distribution. An attempt is made to explain the difference and similarity between alumina insulators and bauxite insulators by taking into account phase composition, porosity, densification degree, and so on. It is a complementary information to elucidate the relationship between microstructure and property. The other purpose of this study is to provide a useful reference to peers in the field of insulator fabrication.

2. Experimental procedure

2.1. Specimens

The specimens studied include three high strength insulators:

Specimen NGK: 400 kN level alumina insulator produced by the world famous porcelain insulator company NGK (Japan).
Specimen BJ: 400 kN level bauxite insulator produced by Bijie Porcelain Insulator Company (Guizhou province, China).
Specimen SZ: 400 kN level bauxite insulator produced by Suzhou Porcelain Insulator Company (Jiangsu province, China).

According to the IEC 672-3 standard, they all belong to the C130 group (high strength insulators) and the bending strength of which must reach 140 MPa for unglazed bar and 160 MPa for glazed bar at least. Although the amount of specimens is limited, they are representatives since they were chosen randomly from each batch and the manufacturers must stabilize the process, composition and property of products for safety.

2.2. X-ray diffraction analysis

A piece of each specimen was crushed and finely ground with a pestle in an agate mortar. The diffraction patterns were recorded with a diffractometer (model: D/Max 2000, Japan), using nickel filtered Cu Kα radiation ($\lambda = 1.54178$ Å). The data was collected in the 2θ range of 2–70°, in the mode of step-scanning with 0.04° in step size and a counting time of 5 s per step. Working voltage and current were 40 kV and 30 mA, respectively. The identification of crystal phase in the specimens was performed by comparing the pattern of the sample with standard pattern of the phase possible to form in the specimens.

2.3. Scanning electron microscopy observation

A small piece of specimen was cut from each insulator and ground with abrasive papers of different fineness in the order of 120 #, 400 #, 800 #, 1200 # and 2000 #. Then the specimen was polished with polishing paper accompanying with diamond paste (2.5 μm). Finally the specimen was etched with a solution containing 20 vol% HF for 20 s and coated with a carbon layer for crystal phase observation. The microstructure observation was done on a scanning electron microscope (model: JSM-6490LV, Japan).

2.4. Porosity calculation

Based on the assumption that pores were homogeneously distributed in the body, the porosity of specimens was measured by the area percentage of pores. To begin with, one needs to choose a representative SEM photograph of specimens and a mesh photograph which could be created by MATLAB. Secondly, one needs to overlay the SEM photograph of specimens with the mesh photograph in PHOTOSHOP. Thirdly, one needs to regulate the opacity of the mesh photograph so as to divide the SEM photograph into many grids. Finally, one could calculate the total grid number of the SEM photograph and count the grid number of pores. Fig. 1 is the porosity calculation schematic diagram. The porosity (P) of specimens is expressed as follows:

$$P = N_1/N \quad (2)$$

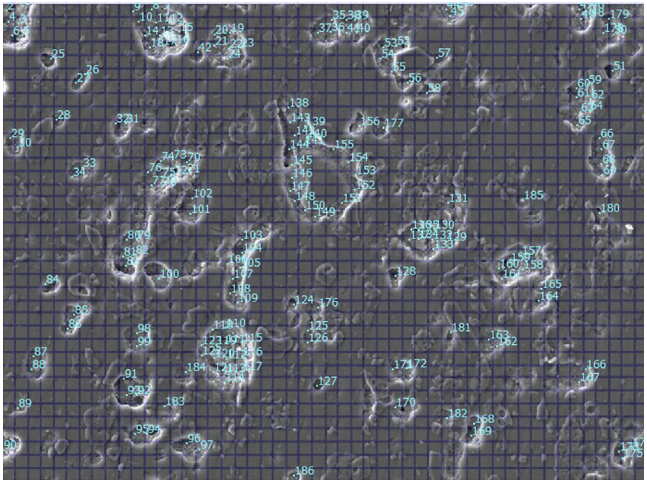

Fig. 1. Porosity calculation schematic diagram.

where N_1 is the grid number of the pores, and N is the total grid number of the SEM photograph selected.

When taking a picture for porosity calculation, the magnification of the picture should be appropriate relative to the size of pores. If the magnification is too large relative to most of the pores, the porosity calculated is not representative and hardly equal to the porosity of the body. If the magnification is too small with respect to most of the pores, the pores are too obscure to measure. Both the cases mentioned above could not get the porosity of a material accurately. This method used above could be adopted for other measurement. But it has a few limitations. For example, if the microstructure measured is indistinguishable by naked eyes, this method is inoperative.

2.5. Density determination

The bulk density of each specimen was calculated by Archimedes method. The measurement includes two steps: mass measurement with an electronic scale and volume measurement with a measuring cylinder. In order to improve the reliability of the data measured, each item was measured five times and the average was taken.

3. Results and discussion

3.1. XRD analysis

The XRD patterns of specimens NGK, SZ and BJ are shown in Fig. 2. The qualitative analysis results show that the three specimens are mainly composed of corundum (PDF#83-2080), mullite (PDF#79-1458), quartz (PDF#46-1045) and feldspar (PDF#76-1238) as well as amorphous phase.

The semi-quantitative analysis of the specimens was carried out with the software JADE 5 in the order of background correction, smoothing, amorphous peak fitting, crystal peak fitting and calculation. The content of amorphous phase is related to the area ratio of the hump to the total area of the pattern [13,14]. The total content of crystal phase equals to the rest of 100% deducting the content of amorphous phase. The

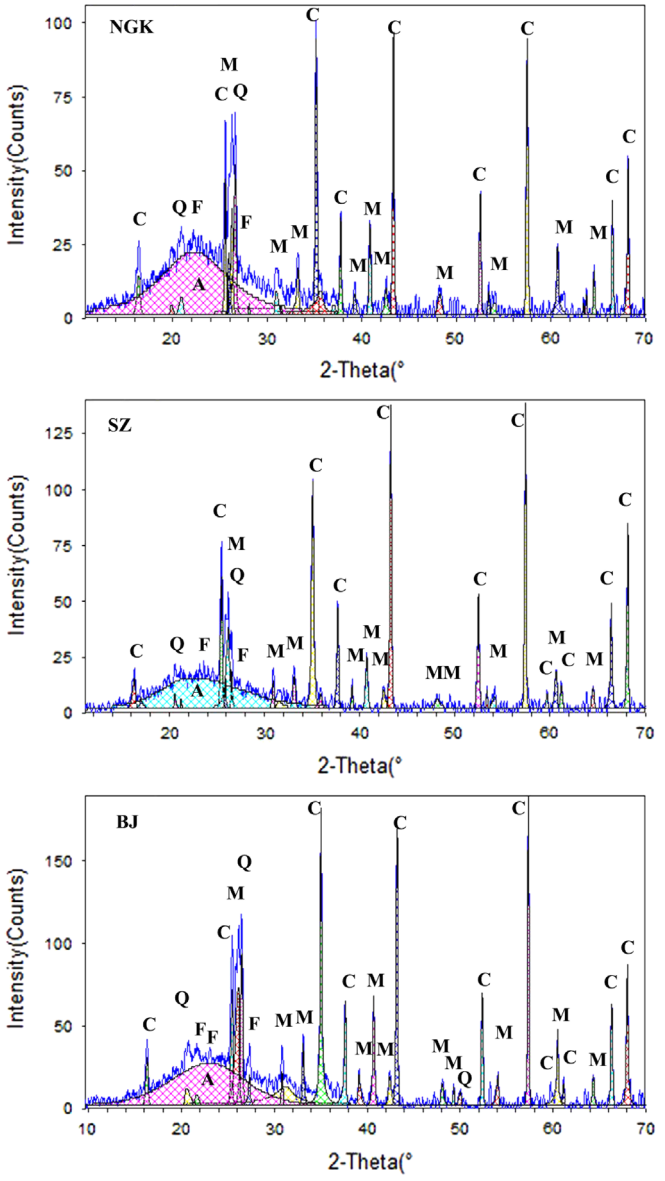

Fig. 2. XRD pattern of samples NGK, SZ and BJ processed with JADE 5; C: corundum; M: mullite; Q: quartz; F: feldspar; and A: amorphous phase.

content of each crystal phase contained in the body of specimens was calculated by the K-value method. The formula is expressed as follows:

$$W_i = W\frac{I_i/K_i}{\sum_i^n I_i/K_i} \tag{3}$$

where W_i is the content of phase i, W is the total content of crystal phase, I_i is the intensity of the strongest peak of phase i, n is the number of composition phase, K_i is the RIR value of phase i which could be obtained from PDF cards or experience. In this calculation, the RIR value for corundum (PDF#83-2080), mullite (PDF#79-1458), quartz (PDF#46-1045) and feldspar (PDF#76-1238) is 1, 0.85, 3.41 and 0.6, respectively. The semi-quantitative analysis results of the three specimens are shown in Fig. 3. Minor phase such as cristobalite was ignored. The two bauxite insulators are close

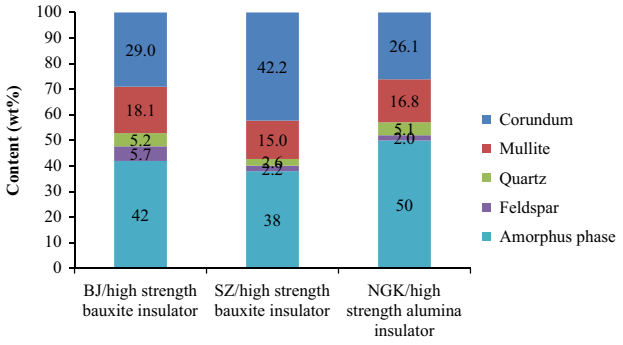

Fig. 3. XRD semi-quantitative analysis results of specimen NGK, specimen SZ and specimen BJ.

in the total content of crystal phase (58 wt% for specimen BJ and 62 wt% for specimen SZ), while different in the content of corundum. In terms of the phase composition, the major difference between bauxite insulators and alumina insulators is the total content of the crystal phase. Specimen NGK has the lowest content of crystal phase (50 wt%) and corundum (26.1 wt%). The three specimens are close in the content of mullite. The content of each phase in specimen SZ is close to that in the C130 high strength bauxite insulator of Siemens reported by Liebermann [15].

3.2. Pores and porosity

Pores are inevitable in the body of insulators because of the decomposition of organic and inorganic compounds in raw material such as carbonate and sulfate as well as other reasons. The pore size, shape and distribution as well as total porosity are of great importance on the property of insulators. The pore condition of specimens NGK, SZ and BJ is showed in Fig. 4.

Most of the pores in specimen NGK are circular or quasi-circular, with a size range of < 30 μm, and homogeneously distributed in the body. There seldom exists interconnected pore or large pore. The total porosity of specimen NGK measured by the method above is 8.9%. The pores in specimen SZ are various in shape such as circular, elliptical and irregular. Most of the pores are within the size range of < 35 μm. Large pores with a size above 40 μm and a few clusters of pores are observable. The total porosity of specimen SZ measured by the method above is 11.3%. The shape of the pores in specimen BJ is similar to that of specimen SZ. Most of the pores are within the size range of < 35 μm. Large pores with a size above 40 μm are observable. Irregular pores, interconnected pores and pore cluster are common. The total porosity of specimen BJ measured by the method above is 10.5%.

For the pore condition, the major difference between alumina insulators and bauxite insulators is that, most of the pores in alumina insulators are circular or quasi-circular while that in bauxite insulators are various such as circular, elliptical and irregular; large pores with a size above 40 μm and a few clusters of pores are observable in bauxite insulators, while that is rare in alumina insulators; the size and distribution of

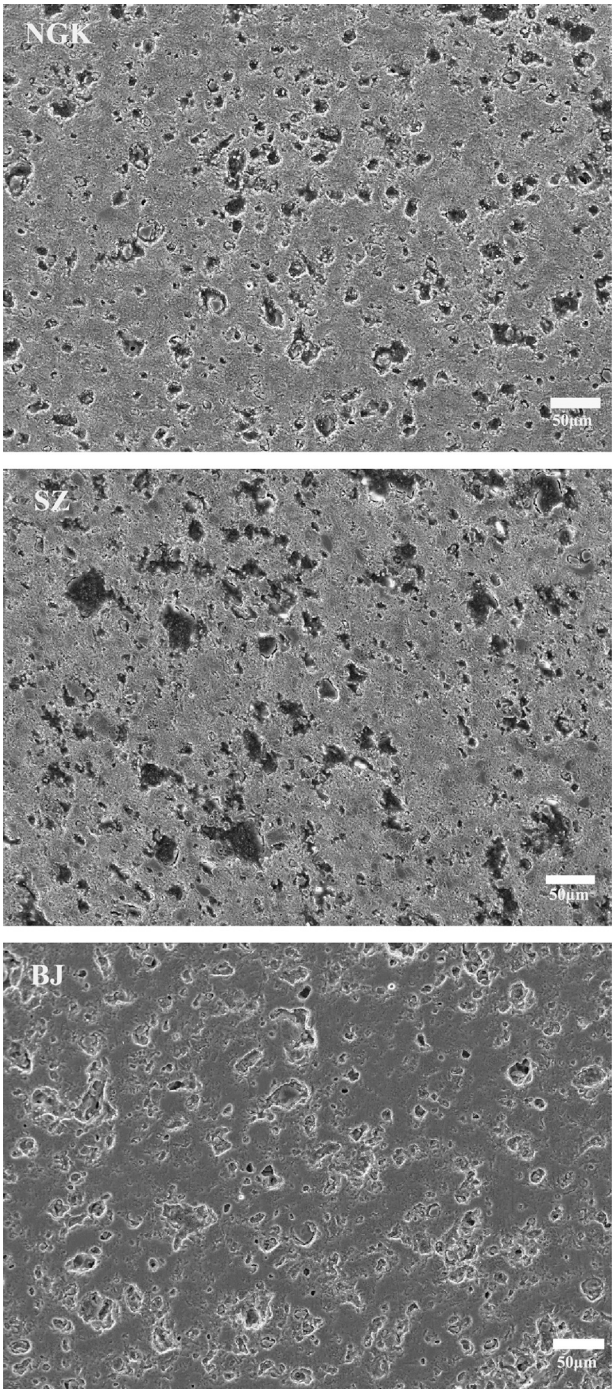

Fig. 4. SEM micrograph of pores in specimens NGK, SZ and BJ.

pores in alumina insulators are more homogeneous than that in bauxite insulators; the porosity of the alumina insulator is the lowest among the three insulators.

It is reported that [16] circular and uniformly distributed pores have a positive effect on the mechanical strength of material, while irregular pore have a stress concentration around the pore when loading which will serve as the fracture origin. In this point, alumina insulators have an advantage over bauxite insulators.

Table 1
Density of the three specimens.

	NGK	BJ	SZ
Density (g/cm^3)	2.80	2.60	2.58

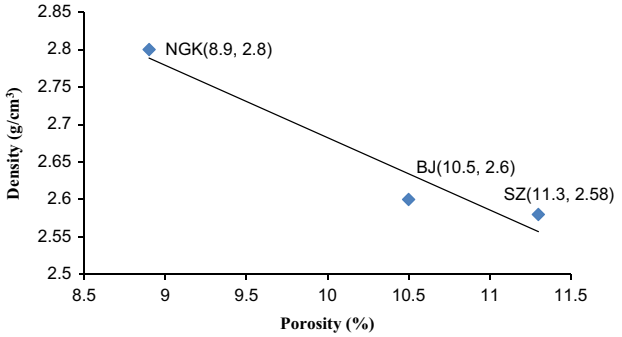

Fig. 5. Relationship between density and porosity.

3.3. Relationship among porosity, amorphous phase and density

The existence of pores in the body of insulators directly hinders the densification of the body resulting in the decrease of efficient loading area and dielectric property. The denser the material is, the higher is the mechanical strength. In this point, material density is of great importance on the mechanical strength [17].

The densities of the three specimens are shown in Table 1. The density of specimen NGK is the maximum (2.80 g/cm^3), while that for specimens BJ and SZ are 2.60 g/cm^3 and 2.58 g/cm^3, respectively. According to the XRD quantitative analysis result, specimen SZ has the lowest content of amorphous phase and the maximum content of corundum, while its density is the lowest. On the contrary, specimen NGK has the maximum content of amorphous phase and the highest density among the three specimens. The relationship between density and porosity is presented in Fig. 4. Although the three specimens came from different plants, underwent different process route as well as had different phase contents, it is very evident that the density of insulators has a negative relationship with the porosity. To sum up, the porosity of insulators is of great influence on the density of insulators, and the use of calcined bauxite observably increases the total porosity of insulators. Besides, there exists a negative linear relationship between the porosity and the content of amorphous phase (Fig. 5). The reason behind this might be that the amorphous phase is composed by low melting point substances and has a low viscosity when sintering, which could fill the pores in the body of insulators [18,19]. To some extent, the more the content of amorphous phase is, the lower is the porosity of the body Fig. 6.

3.4. Corundum particle analysis

Both in alumina insulators and bauxite insulators, corundum particle is the major crystal phase. Corundum has high Young's

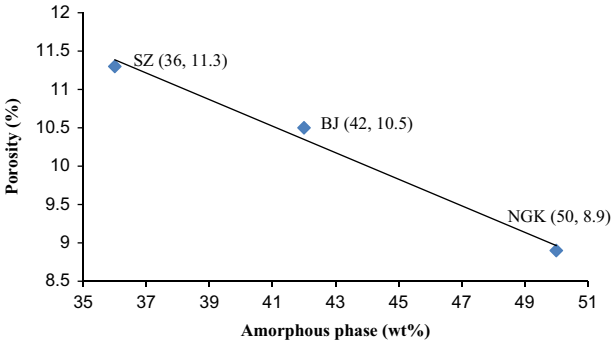

Fig. 6. Relationship between porosity and amorphous phase.

modulus, high hardness and high melting point as well as low expansion coefficient. It is the ideal mineral composition improving the strength of insulators [4,6]. During the sintering process, corundum hardly melted since the sintering temperature (around1300 °C) of insulators is lower than its melting temperature (about 2000 °C). As a result, it remained in the body of insulators, serving as hard barrier, thereby causing the deflection of crack when loading, namely, dispersion strengthening [16,20].

Most of the corundum particles in bauxite insulators are irregular, with a size range of < 20 μm (Fig. 7), and there occasionally exist a few large corundum particles or particle cluster especially in specimen BJ. A typical characteristic of the corundum particle in bauxite insulators is that many corundum particles are porous (Fig. 7). The reason may trace back to the technology of bauxite calcining. Because of the small pores existing in the corundum particles, it could absorb water or gas in the state of green body. When temperature increases, water will vaporize and gas in the pore will diffuse and expand, which facilitates the formation of pores. This may be one of the reasons why specimen SZ has the largest amount of corundum, while it has the lowest density and the maximum porosity among the three specimens.

Most of the corundum in alumina insulators is columnar and dense, with a size range of < 10 μm, and the distribution of which is really homogeneous in the body of alumina insulators (Fig. 7). There seldom exist abnormal corundum particles in the body of alumina insulators.

Generally, the size and distribution of corundum in alumina insulators is more reasonable than that of bauxite insulators, which is another advantage of alumina insulators over bauxite insulators.

3.5. Mullite crystal analysis

Both primary and secondary mullites were observable in bauxite insulators and alumina insulators (Fig. 8). Primary mullite ($3Al_2O_3 \cdot 2SiO_2$) resulted from the transformation of metakaolin, pyrophyllite, etc., is short and dense, while secondary mullite ($2Al_2O_3 \cdot SiO_2$) resulted from the reaction between melt and clay relics is needle-like and interlocking [1,2,11]. The size of secondary mullite is more uniform in specimen SZ than that in the other two specimens. The secondary mullite in specimen NGK is diverse in

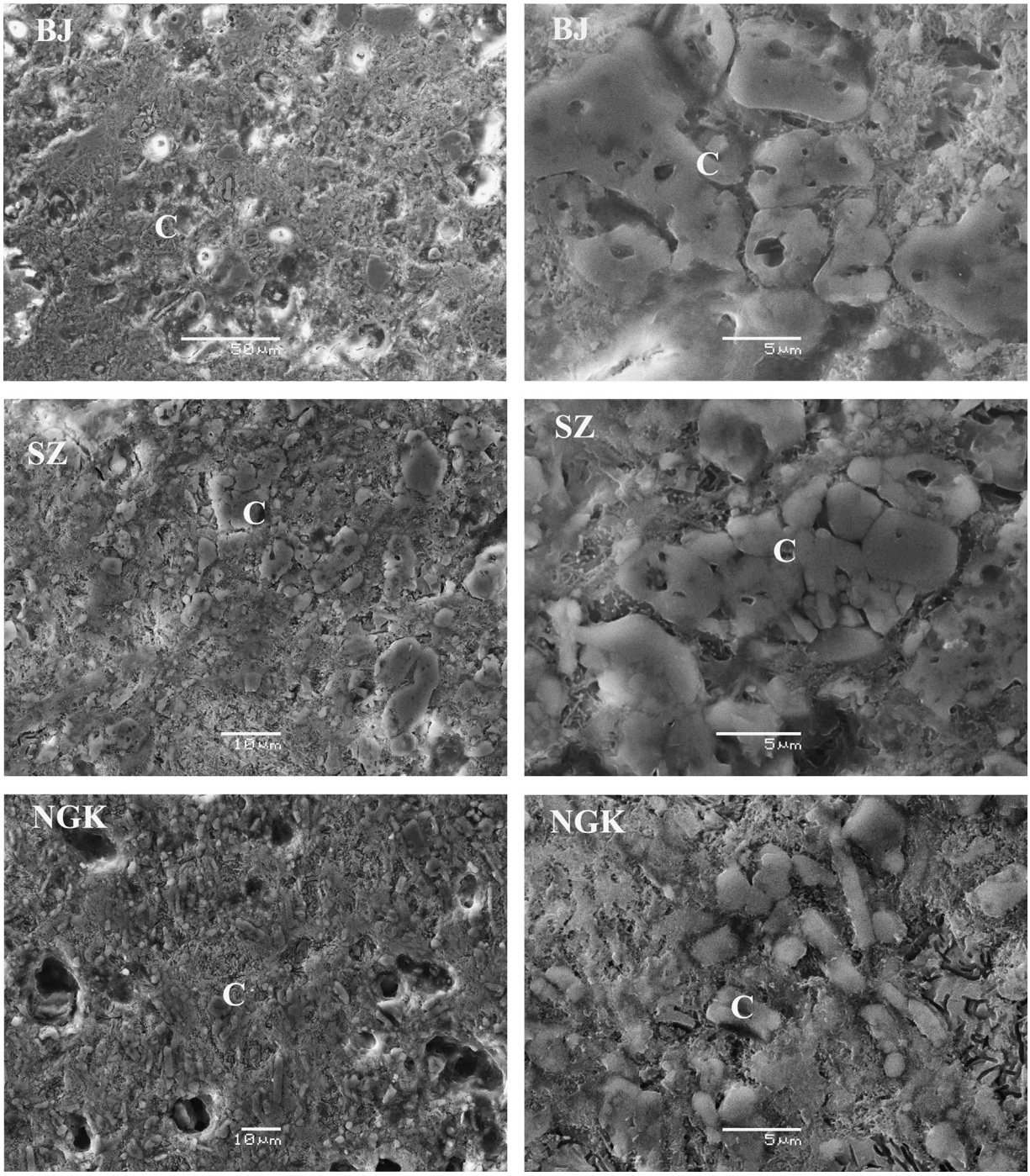

Fig. 7. SEM micrograph of corundum in specimens NGK, SZ and BJ; the left column was taken at low magnification; the right column was taken at high magnification.

sizes, and some crystals are of high aspect ratio. This indicates that the mullite crystal grows well in specimen NGK.

The body of insulators could be regarded as a composite of glass phase, mullite, corundum, etc. Glass serving as the continuous phase is of a low mechanical strength. It is the weak part of the body. Mullite, especially secondary mullite of high aspect ratio, which is needle-like and interlocking, usually appears within the glass phase. It has high bending strength (about 100 MPa) and similar thermal expansion coefficient with the glass phase (4.5×10^{-6} for mullite, 3.0×10^{-6} for glass) [15]. It could improve the strength of glass phase and has a better compatibility with glass phase. So mullite is of great importance on the property of insulators [21,22].

3.6. Microcrack

A common phenomenon was observed from the SEM micrographs (Fig. 9) of the three specimens, i.e., microcrack

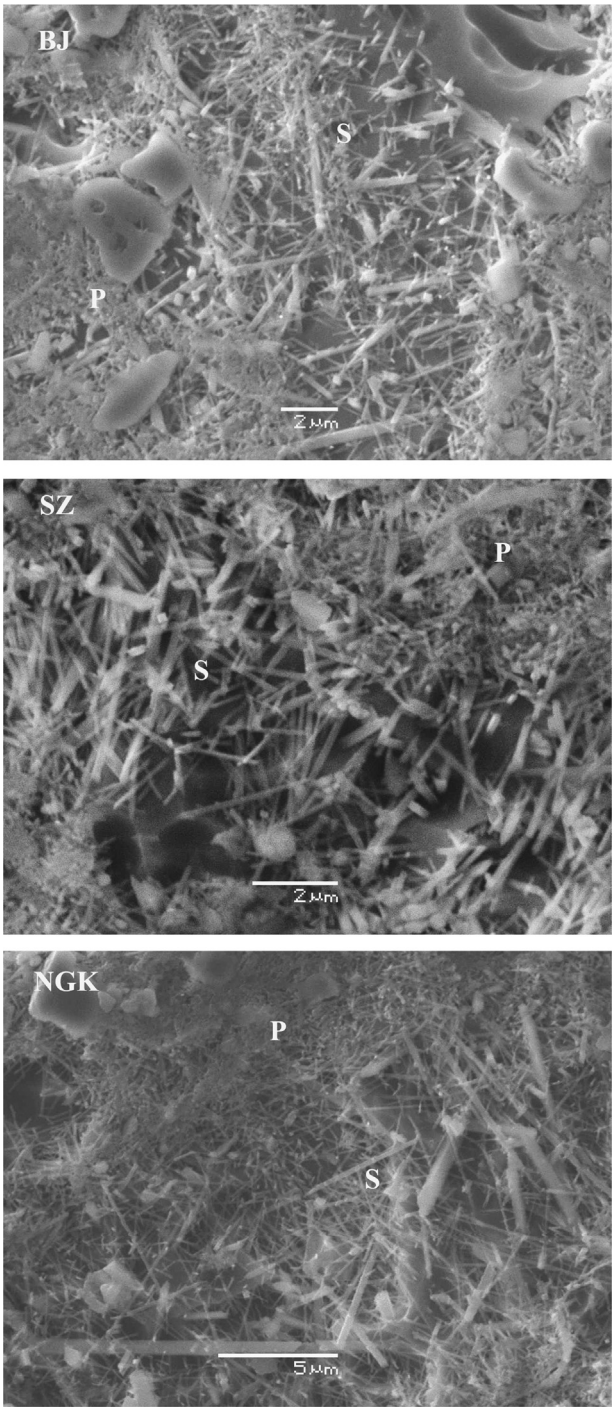

Fig. 8. SEM photograph of mullite in specimen NGK, SZ and BJ.

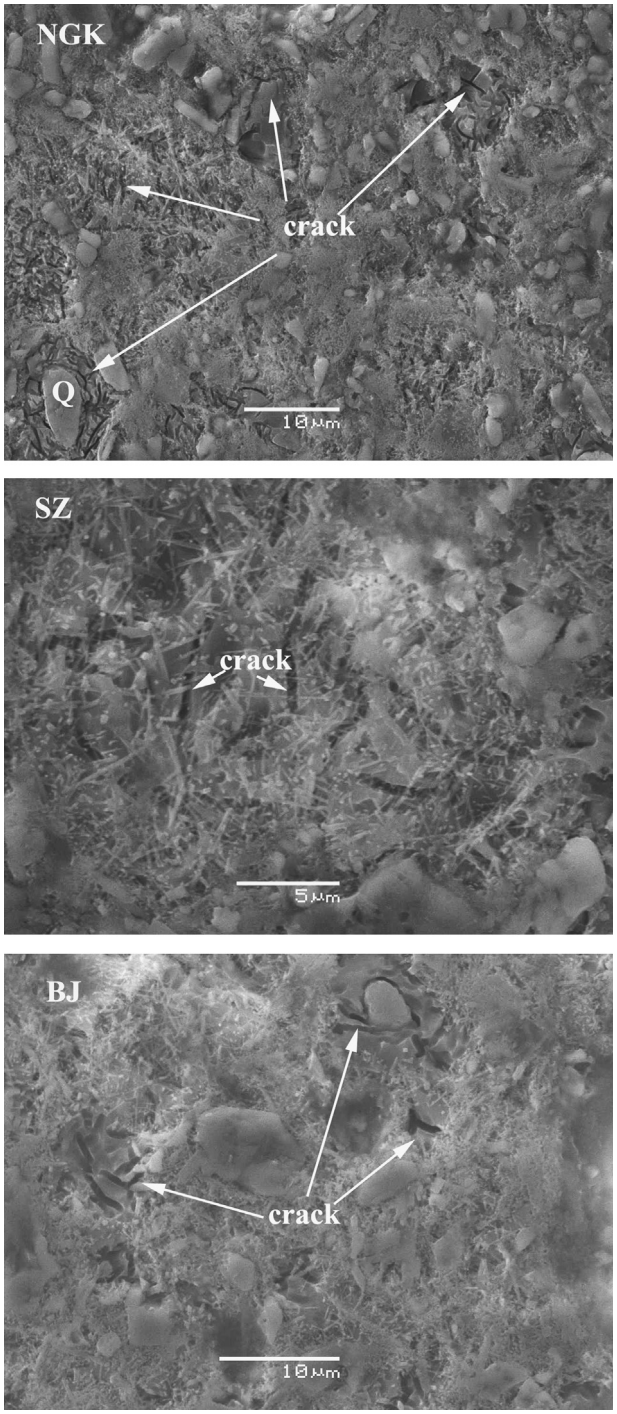

Fig. 9. SEM photograph of crack in specimens NGK, SZ and BJ; Q: quartz.

within 0.5 μm in width usually appeared in vitrified area as well as area around quartz particle. Crack is more obvious in the area without mullite (Fig. 9). The reason might be that vitrified area usually contains more amount of alkaline or alkaline earth element which could lower the sintering temperature than other area. During the cooling process, the solidification of vitrified area is later than area around it. The vitrified area will contract when cooling from liquid state, but there is no enough melt to offset the volume reduction caused by cooling since the area around the melting area is solidified. As a consequence, inner-stress causes the appearance of cracks. As for crack around quartz particle, the reason is that there exists a significant β–α phase transformation of quartz particle at 573 °C during the cooling process, causing volume jump (volume reduction 2% relative to the precursor) [11]. As a result, inner-stress gives rise to circumferential cracks around the quartz particle. Why crack is more obvious in the area without mullite? The reason might trace back to the nature of mullite: high strength, acicular and interlocking morphology.

Among the three specimens, cracks in specimen NGK are more obvious than that in the two other specimens, which is a disadvantage of alumina insulators. The reason behind this might be that the contraction of specimen NGK was more serious during the cooling process than that of the two other specimens since it has the maximum content of amorphous phase.

4. Conclusions

A comparative study has been carried out on two kinds of high strength porcelain insulators by XRD, SEM and ceramography. From the analysis above, we could draw a few conclusions as follows.

Porosity has a negative linear relationship with the content of amorphous phase. To some extent, the more the content of amorphous phase is, the lower is the porosity of the body. Porosity is the major factor influencing the density of porcelain insulators, which has a negative relationship with the density of the body. Compared with alumina, the calcined bauxite used as a raw material will cause the increase of porosity. Microcracks usually appear in vitrified area and area around quartz particle where mullite is rare, crack is obvious. Generally, the size and distribution of microstructures such as corundum particles and pores are more homogeneous in alumina insulators than that in bauxite insulators. Decreasing the amount of quartz in raw material and increasing the amount of mullite in vitrified area could improve the mechanical strength of porcelain insulators further.

Acknowledgment

This work is supported by the National Science and Technology Supporting Plan (Grant no. 2009BAF43B00), Academy-Region Cooperation Project of Chinese Academy of Sciences (Grant no. 2009-5-27).

References

[1] N. Montoya, F.J. Serrano, M.M. Reventós, J.M. Amigo, J. Alarcón, Effect of TiO_2 on the mullite formation and mechanical properties of alumina porcelain, J. Eur. Ceram. Soc. 4 (2010) 839–846.
[2] Y. Meng, G. Gong, Z. Wu, Z. Yin, Y. Xie, S. Liu, Fabrication and microstructure investigation of ultra-high-strength porcelain insulator, J. Eur. Ceram. Soc. 12 (2012) 3043–3049.
[3] V.T. Kontargyri, L.N. Plati, I.F. Gonos, I.A. Stathopulos, Measurement and simulation of the voltage distribution and the electric field on a glass insulator string, Measurement 5 (2008) 471–480.
[4] J. Liebermann, W. Schulle, Bauxitic porcelain – a new high-tech product for high-voltage insulation, Key Eng. Mater. (2002) 1727–1730.
[5] J. Liebermann, New effective ways toward solving the problem of contamination of porcelain insulators, Refract. Ind. Ceram. 1-2 (2002) 55–64.
[6] J. Liebermann, Microstructure properties and product quality of strength-stressed high-voltage insulators, Am. Ceram. Soc. Bull. 2 (2003) 39–46.
[7] R.H. Piva, P. Vilarinho, M.R. Morelli, M.A. Fiori, O.R.K. Montedo, Influence of Fe_2O_3 content on the dielectric behavior of aluminous porcelain insulators, Ceram. Int. 7 (2013) 7323–7330.
[8] I.A. Metwally, A. Al-Maqrashi, S. Al-Sumry, S. Al-Harthy, Performance improvement of 33 kV line-post insulators in harsh environment, Electr. Pow. Syst. Res. 9-10 (2006) 778–785.
[9] J.M. Amigó, F.J. Serrano, M.A. Kojdecki, J. Bastida, V. Esteve, M.M. Reventós, F. Martí, X-ray diffraction microstructure analysis of mullite, quartz and corundum in porcelain insulators, J. Eur. Ceram. Soc. 9 (2005) 1479–1486.
[10] J. Amigó, X-ray powder diffraction phase analysis and thermomechanical properties of silica and alumina porcelains, J. Eur. Ceram. Soc. 1 (2004) 75–81.
[11] R.A. Islam, Y.C. Chan, M.F. Islam, Structure–property relationship in high-tension ceramic insulator fired at high temperature, Mater. Sci. Eng. B 2 (2004) 132–140.
[12] M. Touzin, D. Goeuriot, C. Guerret-Piécourt, D. Juvé, H.J. Fitting, Alumina based ceramics for high-voltage insulation, J. Eur. Ceram. Soc. 4 (2010) 805–817.
[13] F. Tarasi, M. Medraj, A. Dolatabadi, J. Oberste-Berghaus, C. Moreau, Amorphous and crystalline phase formation during suspension plasma spraying of the alumina–zirconia composite, J. Eur. Ceram. Soc. 15 (2011) 2903–2913.
[14] I. Ganesh, J.M.F. Ferreira, Influence of raw material type and of the overall chemical composition on phase formation and sintered microstructure of mullite aggregates, Ceram. Int. 5 (2009) 2007–2015.
[15] J. Liebermann, Microstructure properties and product quality of strength-stressed high-voltage insulators, Am. Ceram. Soc. Bull. 2 (2003) 39–46B.
[16] G. Stathis, Effect of firing conditions, filler grain size and quartz content on bending strength and physical properties of sanitaryware porcelain, J. Eur. Ceram. Soc. 8 (2004) 2357–2366.
[17] M.M. Jordan, M.A. Montero, S. Meseguer, T. Sanfeliu, Influence of firing temperature and mineralogical composition on bending strength and porosity of ceramic tile bodies, Appl. Clay Sci. 1–2 (2008) 266–271.
[18] F. Torres, J. Alarcon, Effect of MgO/CaO ratio on the microstructure of cordierite-based glass–ceramic glazes for floor tiles, Ceram. Int. 5 (2005) 683–690.
[19] L. Carbajal, F. Rubiomarcos, M. Bengochea, J. Fernandez, Properties related phase evolution in porcelain ceramics, J. Eur. Ceram. Soc. 13–15 (2007) 4065–4069.
[20] D. Hasselman, R. Fulrath, Proposed fracture theory of a dispersion-strengthened glass matrix, J. Am. Ceram. Soc. 2 (1966) 68–72.
[21] S. Deniel, N. Tessier-Doyen, C. Dublanche-Tixier, D. Chateigner, P. Blanchart, Processing and characterization of textured mullite ceramics from phyllosilicates, J. Eur. Ceram. Soc. 12 (2010) 2427–2434.
[22] W.E. Lee, D.D. Jayaseelan, S. Zhang, Solid–liquid interactions: the key to microstructural evolution in ceramics, J. Eur. Ceram. Soc. 7 (2008) 1517–1525.